

Effect of embedded microcrystallites on the light-induced degradation of hydrogenated amorphous silicon

Yoram Lubianiker and J. David Cohen

Department of Physics, University of Oregon, Eugene, Oregon 97403

Hyun-Chul Jin and John R. Abelson

Department of Materials Science and Engineering and the Coordinated Science Laboratory, University of Illinois, Urbana, Illinois 61801

(Received 8 September 1998; revised manuscript received 22 March 1999)

We have studied the degradation kinetics of undoped hydrogenated amorphous silicon (a -Si:H) samples, in which a small fraction of microcrystallites is embedded. We find that the defect density increases with an unusually slow initial pace, which is then followed by the “normal” $t^{1/3}$ law and the subsequent saturation. The corresponding photoconductivity shows a remarkable initial stability. We present a model that reproduces the experimental results, and relates the structural and degradation anomalies. The measured defect density is interpreted as a superposition of contributions from a defective layer that wraps the microcrystallites and a high-quality amorphous matrix. [S0163-1829(99)11531-5]

The widespread application of photovoltaic cells based on hydrogenated amorphous silicon (a -Si:H) is greatly impeded by the degradation of the material due to prolonged exposure to light, known as the Staebler-Wronski effect (SWE).¹ The most significant consequence of such exposure is the creation of metastable dangling bonds (DB's), following a well documented time and light intensity dependence.² It is known that a -Si:H solar cells grown under hydrogen dilution are more stable,³ and it has been recently argued that this is related to the onset of silicon microcrystallite formation within the amorphous material.⁴ The more stable material can be thus viewed as an intermediate state between pure a -Si:H and microcrystalline silicon, the latter of which is known⁵ to be stable. However, there have been only a few studies of the degradation kinetics of a -Si:H films in this intermediate region. In this report, we examine the degradation kinetics of undoped a -Si:H films that contain a small fraction of microcrystallites. The films exhibit an abnormal degradation kinetics, that can be accounted for by a model that incorporates the mixed phase nature of the material.

The a -Si:H samples used in this study were deposited by dc reactive magnetron sputtering of a $5'' \times 12''$ planar Si target in an Ar+H₂ plasma.⁶ The argon pressure was 1.5 mTorr and the hydrogen pressure was 0.6 mTorr. The samples were simultaneously grown on p^+ c -Si and on Corning 7059 glass. The substrates were kept at a temperature of 230 °C, and the growth rate was about 170 Å/min. For the capacitance measurements we evaporated semitransparent Pd dots on top of the a -Si:H/ c -Si films. For the films grown on glass we evaporated Cr contacts in a coplanar configuration, thus obtaining approximately ohmic contacts, which are suitable for measurements of the secondary photoconductivity. Prior to the measurements the samples were annealed at 490 K for 1 h. Light soaking was performed using a tungsten-halogen lamp, with a maximal intensity of 4.5 W/cm², with the samples immersed in methanol, to maintain a surface temperature below 60 °C.

To verify the presence of microcrystallites in our films we measured the subband-gap absorption spectrum using tran-

sient photocapacitance and transient photocurrent spectroscopies.⁷ The results are presented in Fig. 1, together with a representative spectrum for pure a -Si:H. The photocurrent curve essentially resembles the absorption spectrum of microcrystalline silicon, while the photocapacitance curve consists of a typical a -Si:H absorption curve on top of which an extra feature at ~ 1.2 eV is superimposed. Such absorption curves⁸ indicate the inclusion of a small volume fraction of microcrystallites in the a -Si:H film. This is confirmed by our Raman measurements, which show an additional “shoulder” at 522 cm⁻¹, and by TEM micrographs of such films.⁸

To study the degradation kinetics we determined the defect density using drive-level capacitance profiling (DLCP)

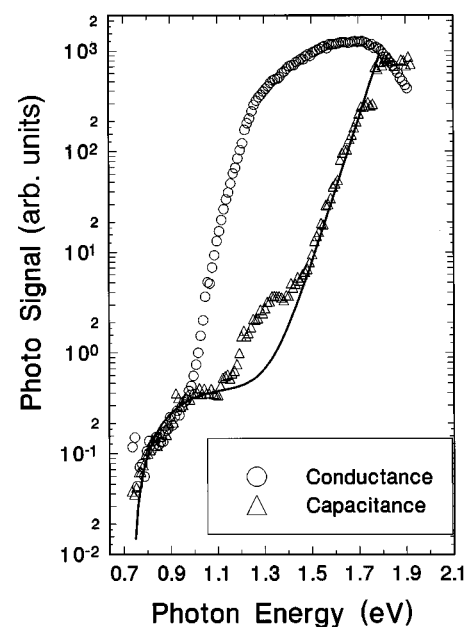


FIG. 1. Subband-gap absorption spectra as determined from the transient photocapacitance and transient photocurrent experiments. The solid line represents a typical spectrum for a pure a -Si:H sample.

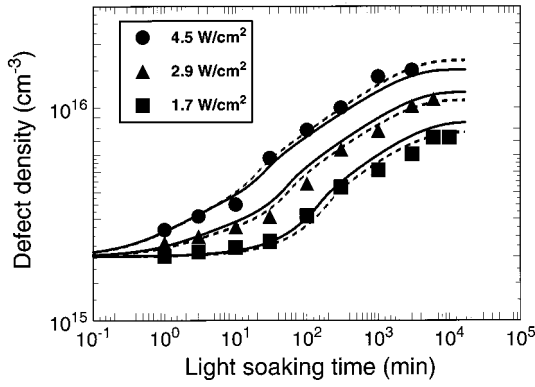


FIG. 2. The defect density as a function of the light soaking time. The lines represent model fittings without (full) and with (dashed) changing C_1 as a function of the generation rate (see text).

measurements.⁹ These were performed at 350 K (at a frequency of 11 Hz) to avoid thermal annealing effects. In Fig. 2 we present the defect densities as a function of light soaking time under three different intensities. Starting with the high-intensity curve, we see that initially the defect density increases very slowly, for about 10 min (hereafter called “stage 1”). We note, however, that even after 1 min of light soaking the defect density is higher than its annealed state value of $2 \times 10^{15} \text{ cm}^{-3}$. After this stage of slow degradation, the defect density increases dramatically in the next time interval (“stage 2”), and later at a more moderate pace (“stage 3”) followed by saturation (“stage 4”). All these behaviors, including the abrupt increase in stage 2, were completely reproducible. Turning to the degradation under lower light intensities we observe the same qualitative features, except that stage 1 becomes even slower as the light intensity decreases, while stage 2 is gradually suppressed. It is noteworthy that the transition point from stage 1 to stage 2 occurs at longer times and lower defect densities as the light intensity is reduced. The other differences between the curves, i.e., the lower overall defect density and the longer times required to achieve saturation under lower light intensity, are well known and generally occur for all $a\text{-Si:H}$ samples.² The annealing kinetics of our samples were examined in consecutive isochronal steps of 15 min at increasing temperature. These data could be fitted by a single activated process, suggesting the existence of a only single type of light-induced defect.

The degradation of $a\text{-Si:H}$ is commonly explained² as a consequence of nonradiative tail to tail recombination that produces metastable DB’s in addition to those present at equilibrium. This process is eventually balanced by light-induced annealing, which is attributed¹⁰ to electron trapping into DB’s. Thus, one can write a kinetic equation for the DB density N as

$$\frac{dN}{dt} = C_{\text{sw}} \frac{G^2}{N^2} - \lambda G. \quad (1)$$

The coefficients C_{sw} and λ control the creation and annealing of DB’s, respectively, G is the photocarrier generation rate, and t is the light soaking time. We have neglected thermal effects due to the low-surface temperature of the sample during light soaking (see above). This model assumes that most

of the recombination traffic is through the DB’s, leading to the N^{-2} dependence of the creation term. An approximate solution of Eq. (1) yields the commonly observed behavior of $N(t) \propto G^{2/3} t^{1/3}$, which is quite different from our experimental findings. We further note that the disagreement between the above model and our results cannot be attributed to an additive constant resulting from stable defects within or around the microcrystallites. Rather, the presence of the microcrystallites leads to an altogether different degradation kinetics. We present below a modification of the theoretical model that accounts for these differences without assuming fundamentally different mechanisms for the creation and annealing of DB’s.

We believe that the observed behavior requires a second degrading phase, and thus, propose that inside the high-quality amorphous silicon film (phase 1) there are microcrystallites (phase 3), which are surrounded by a highly defective amorphous silicon layer (phase 2). Phase 2, which may also include grain boundary states, can be thought of as a tissue layer that wraps the embedded microcrystallites. While our model consists of three phases, only the two amorphous phases can degrade. Supporting evidence for this proposed structure has been given independently by transport measurements¹¹ and by subband-gap absorption¹² studies performed on films that contained a much higher fraction of microcrystallites. The latter work also showed that the defective amorphous layer contains a high-hydrogen concentration (around 38% hydrogen, whereas a “normal” value for $a\text{-Si:H}$ is about 10%).

For such a structure the overall measured defect density will be given by a superposition of the contributions of the different phases with their relative volume fraction (f_i , where i signifies the phase number) as a weighting function. Since the defect density contributed by the microcrystalline phase is expected only to contribute a small overall constant we have set this defect density to zero. For phase 2, we can express the kinetics of the increase of its defect density N_2 using Eq. (1) with C_2 and λ_2 as the creation and annealing coefficients in this phase, respectively. We also note that due to the high-initial defect density of this phase, N_2 is expected to increase only slightly and relatively slowly upon light soaking.

Turning to the first phase, we assume that in state A a significant fraction of the photocarriers diffuse from phase 1 into the defective phase 2, and recombine there. We denote by Z density of N_2 states that control the recombination of carriers from phase 1. Accordingly, we obtain the kinetic equation

$$\frac{dN_1}{dt} = C_1 \frac{G^2}{Z^2} - \lambda_1 \frac{G}{Z} N_1, \quad (2)$$

where C_1 and λ_1 denote the light-induced defect creation and annealing coefficients for phase 1. Due to the high value of Z the degradation term is relatively small, so that for a relatively long time the degradation of this phase will be insignificant. During this “incubation” time N_1 will remain almost a constant, but *the overall defect density will exhibit a small increase* due to the contribution of phase 2. This slow degradation corresponds to stage 1 in the experimental

curves. Following this, recombination in the high-quality phase will gradually shift to its own DB's, *but the lifetimes will remain constant* since an equivalent number of Z states cease to act as recombination centers. This is because the diffusion of carriers from phase 1 to phase 2 decreases as N_1 increases. This will result in a *linear increase* of N_1 with time (stage 2). Eventually, the density of N_1 states will exceed the number of Z states. From this time on, the lifetimes in phase 1 will be determined solely by the density of dangling bonds in phase 1. The degradation will then follow the kinetics of Eq. (1), i.e., the “normal” $t^{1/3}$ law and the subsequent saturation (stages 3 and 4 of the degradation process).

The above discussion explains qualitatively how our model accounts for the entire experimental behavior. In addition, we can fit the experimental data in detail using a reasonable set of parameters, as we show in Fig. 2 (full lines). We obtain satisfactory fits for all the experimental curves simultaneously¹³ by changing only the generation rate (which is determined from the measured light intensity) and the corresponding Z value. In our calculations we have used initial defect densities of $5 \times 10^{14} \text{ cm}^{-3}$ for the high-quality phase and $3 \times 10^{16} \text{ cm}^{-3}$ for the defective phase. It is noteworthy that the value of $N_1(0)$ is lower than in standard *a*-Si:H films. This is necessary to account for the initial low value of the overall defect density, and is consistent with the high performance of solar cells which utilize such a mixed phase material.⁴ We hypothesize that the presence of the microcrystallites leads to a reduction of the strain in the high-quality phase, leading to this exceptionally high-quality material. Indeed, the high quality of the amorphous matrix under such conditions has been noted previously.⁴

By fitting the experimental data we found realistic values of $C_1 = 0.0013 \text{ cm}^{-3} \text{ s}$ and $\lambda_1 = 6 \times 10^{-13}$, while the corresponding values for the defective second phase were determined to be about 10^3 times higher. The relatively low value of C_1 and the high value of C_2 are consistent with the respective high and low quality¹⁴ of the associated phases. The former value also assures that the saturated DB density in phase 1 will be lower than its usual value in pure *a*-Si:H. Since the recombination of photocarriers in state B is restricted to the high quality phase, this predicts an improved saturated performance for a solar cell which utilizes such a mixed phase material. On the other hand, if the concentration of the other phases becomes too high, then these phases will dominate the overall recombination even in state B, and the corresponding solar cell will perform poorly.

The one feature that our model fails to reproduce *quantitatively* is the dependence of the saturated defect density on light intensity. While the model predicts a dependence of $G^{1/2}$, the experimental results represent a somewhat higher exponent of 0.6. The fitting can be significantly improved if we allow C_1 to be slightly dependent on G , as is demonstrated in the dashed lines in Fig. (2). These were calculated by allowing C_1 to increase by 40% as the light intensity was changed by a factor of 2.8. Here, we observe excellent agreement with the experimental data. Such a proposed variation of C_1 with light intensity may indicate the existence of potential fluctuations in the high-quality phase, (e.g., induced by the presence of the microcrystallites) which separate the electrons and holes. When the generation rate increases the

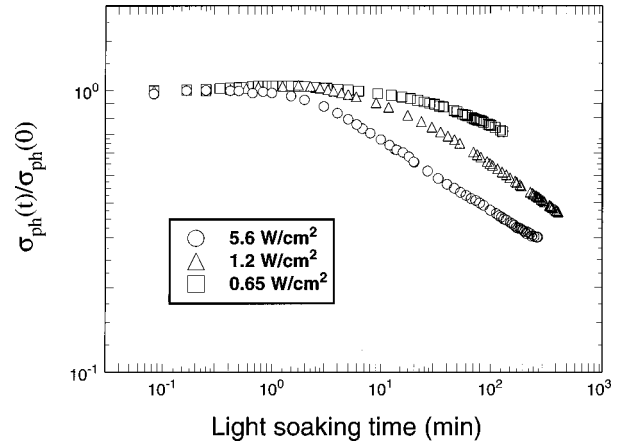


FIG. 3. The normalized photoconductivity as a function of light soaking time.

photocarriers are more likely to overcome these fluctuations and recombine more efficiently, leading to a $C_1(G)$ dependence. This scenario can also account for the $Z(G)$ dependence that we used (i.e., at higher generation rate the photocarriers are more likely to overcome the potential fluctuations and subsequently “see” more of the N_2 states). More experimental data will be needed to verify whether this is indeed the case.

In order to reproduce the relatively long “incubation” time and the accelerated stage 2 of the degradation our model assumes that the recombination in state A is governed by the Z states. It thus predicts that the lifetime of the photocarriers in phase 1 does not significantly degrade until the beginning of stage 3. To test this prediction we measured the effects of degradation on the photoconductivity, σ_{ph} . This was measured in a coplanar configuration using the samples grown on glass. In Fig. 3 we present the normalized photoconductivity as a function of light soaking time. Indeed, we see an anomalous type of degradation: σ_{ph} remains initially constant and starts to decrease only after a few minutes, roughly following a $t^{-1/3}$ law. The time at which σ_{ph} starts to drop becomes longer with decreasing light intensity, and the saturation times were found to be roughly compatible with those of the defect creation. A comparison of Figs. 2 and 3 shows that σ_{ph} remains constant even though the defect density increases. This means that the corresponding metastable defects are created without affecting the lifetime of the photocarriers within the high-quality phase 1 (which dominates the photoconductivity due to its high-volume fraction). Thus, the photoconductivity data provide independent experimental support for our model. The small time difference between the beginning of stage 3 in the DLCP data and the decrease of σ_{ph} is attributed to slight differences in the growth on the different substrates (*c*-Si and glass).

In conclusion, we have studied the degradation kinetics of *a*-Si:H samples which contain microcrystallites in the amorphous network. The most significant deviation of the degradation kinetics from the “normal” behavior is a remarkably slow initial degradation. We have suggested a model that accounts for the complicated experimental results through the existence of two phases of *a*-Si:H: One is of low-quality and high-hydrogen concentration that lies adjacent to the

micro-crystallites, and the other, of very high quality, is the vast majority of the film.

The authors are indebted to R. Lowe-Webb for the Raman measurements and to K. Palinginis for his assistance in the

numerical simulations. The work at Oregon was supported by NREL under Subcontracts Nos. XAN-4-13318-07 and XAF- 8-17916-05, and at Illinois by the Samsung Advanced Institute of Technology.

-
- ¹D. L. Staebler and C. R. Wronski, *Appl. Phys. Lett.* **31**, 292 (1977).
- ²M. Stutzmann, W. B. Jackson, and C. C. Tsai, *Phys. Rev. B* **32**, 23 (1985).
- ³S. Guha, K. L. Narasimhan, and M. S. Pietruszko, *J. Appl. Phys.* **52**, 859 (1981).
- ⁴D. V. Tsu, B. S. Cho, S. R. Ovshinsky, S. Guha, and J. Yang, *Appl. Phys. Lett.* **71**, 1317 (1997).
- ⁵J. Meier, P. Torres, R. Platz, S. Dubail, U. Kroll, J. A. Anna Selvan, N. Pellaton Vaucher, Ch. Hof, D. Fischer, H. Keppner, A. Shah, K.-D. Ufert, P. Giannoules, and J. Koehler, in *Amorphous Silicon Technology*, edited by M. Hack, E. A. Schiff, S. Wagner, A. Matsuda, and R. Schropp, MRS Symposia Proceedings No. 420 (Materials Research Society, Pittsburgh, 1996), p. 3.
- ⁶M. Pinarbasi, M. J. Kushner, and J. R. Abelson, *J. Appl. Phys.* **68**, 2255 (1990).
- ⁷J. D. Cohen, T. Unold, and A. V. Gelatos, *J. Non-Cryst. Solids* **141**, 142 (1992).
- ⁸D. Kwon, H. Lee, J. D. Cohen, H.-C. Jin, and J. R. Abelson, *J. Non-Cryst. Solids* **227–230**, 1040 (1998).
- ⁹C. E. Michelson, A. V. Gelatos, and J. D. Cohen, *Appl. Phys. Lett.* **47**, 412 (1985).
- ¹⁰M. Stutzmann, J. Nunnemkamp, M. S. Brandt, and A. Asano, *Phys. Rev. Lett.* **67**, 2347 (1993).
- ¹¹R. Schwarz, T. Murias, J. P. Conde, P. Brogueira, and V. Chu, in *Amorphous and Microcrystalline Silicon Technology—1998*, edited by R. Schropp, H. M. Branz, M. Hack, I. Shimizu, and S. Wagner, MRS Symposia Proceedings No. 507 (Materials Research Society, Pittsburgh, 1998), p. 799.
- ¹²F. Diehl, B. Schroder, and H. Oechsner, in *Amorphous and Microcrystalline Silicon Technology—1998* (Ref. 11), p. 819. This work also provides estimated sizes for the microcrystallites and the disordered tissue layer.
- ¹³The exact values for all the parameters used for the fitting shown in Fig. 2 for the high intensity curve are: $G = 7.5 \times 10^{22} \text{ cm}^{-3} \text{ s}^{-1}$, $f_1 = 0.95$, $f_2 = 0.05$, $N_1(0) = 5 \times 10^{14} \text{ cm}^{-3}$, $N_2(0) = 3 \times 10^{16} \text{ cm}^{-3}$, $Z = 2.5 \times 10^{15} \text{ cm}^{-3}$, $C_1 = 0.0013 \text{ cm}^{-3} \text{ s}$, $\lambda_1 = 6 \times 10^{-13}$, $C_2 = 5.2 \text{ cm}^{-3} \text{ s}$, $\lambda_2 = 1.8 \times 10^{-9}$. We note that there is some latitude in the choice of these values. However, obtaining a good fit for all light intensities *simultaneously* while keeping the values of the parameters within *reasonable* limits, imposes considerable restrictions on their values.
- ¹⁴In *a*-Si:H the parameter C is usually around $0.1 \text{ cm}^{-3} \text{ s}$, and varies depending on the quality of the material. See, for example, R. Street, *Hydrogenated Amorphous Silicon* (Cambridge University Press, Cambridge, 1991), p. 218.